

Spring 5-30-1961

Angular Distribution of Electrons in Extensive Air Showers

Don D. Laniewski

Follow this and additional works at: https://digitalrepository.unm.edu/phyc_etds



Part of the [Astrophysics and Astronomy Commons](#), and the [Physics Commons](#)

Recommended Citation

Laniewski, Don D. "Angular Distribution of Electrons in Extensive Air Showers." (1961). https://digitalrepository.unm.edu/phyc_etds/132

This Thesis is brought to you for free and open access by the Electronic Theses and Dissertations at UNM Digital Repository. It has been accepted for inclusion in Physics & Astronomy ETDs by an authorized administrator of UNM Digital Repository. For more information, please contact disc@unm.edu.

UNIVERSITY OF NEW MEXICO-UNIVERSITY LIBRARIES



A14429 086539

378.789

Un30^lani

1961

cop. 2



THE LIBRARY
UNIVERSITY OF NEW MEXICO



Call No.

378.789
Un308ani
1961
cop. 2

Accession
Number

274211

FOLLOW COMMENTS
PLEASE

UNIVERSITY OF NEW MEXICO LIBRARY

MANUSCRIPT THESES

Unpublished theses submitted for the Master's and Doctor's degrees and deposited in the University of New Mexico Library are open for inspection, but are to be used only with due regard to the rights of the authors. Bibliographical references may be noted, but passages may be copied only with the permission of the authors, and proper credit must be given in subsequent written or published work. Extensive copying or publication of the thesis in whole or in part requires also the consent of the Dean of the Graduate School of the University of New Mexico.

This thesis by ..Don D. Laniewski.....
has been used by the following persons, whose signatures attest their acceptance of the above restrictions.

A Library which borrows this thesis for use by its patrons is expected to secure the signature of each user.

NAME AND ADDRESS

DATE

MANUSCRIPT TERMS

Unpublished theses submitted to the Faculty and Library are given and deposited in the University of New Mexico Library open for inspection, but are to be used only in the event the rights of the author. Bibliographical references may be made, but passages may be copied only with the permission of the author, and proper credit must be given in subsequent written or published work. Extensive copying or publication of the thesis in whole or in part requires also the consent of the Dean of the Graduate School of the University of New Mexico.

This thesis by Robert H. Taylor has been used by the following persons: Josephine Taylor acceptance of the above conditions.

A library which borrows this thesis and the author is expected to secure the signature of each user.

NAME AND ADDRESS _____ DATE _____

ANGULAR DISTRIBUTION OF ELECTRONS
IN EXTENSIVE AIR SHOWERS

By

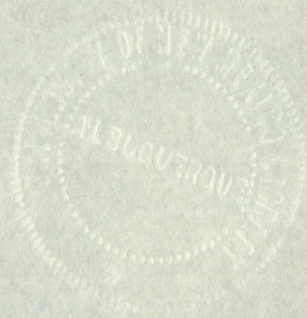
Don D. Laniewski

A Thesis

Submitted in Partial Fulfillment of the
Requirements for the Degree of
Master of Science in Physics

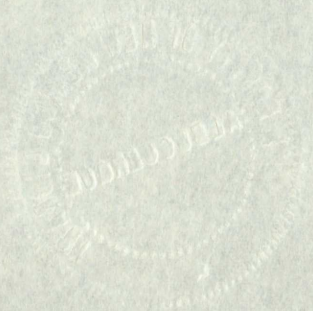
The University of New Mexico

1961



THE UNIVERSITY OF CHICAGO
LIBRARY

ANNUAL REPORT OF THE BOARD OF TRUSTEES
FOR THE YEAR ENDING 1911



THE UNIVERSITY OF CHICAGO

CHICAGO

Submitted in partial fulfillment of the
Requirements for the degree of
Master of Arts in Education

The University of Chicago

1911

This thesis, directed and approved by the candidate's committee, has been accepted by the Graduate Committee of the University of New Mexico in partial fulfillment of the requirements for the degree of

MASTER OF SCIENCE

E. Castetter
Dean

May 30, 1961
Date

**ANGULAR DISTRIBUTION OF ELECTRONS IN
EXTENSIVE AIR SHOWERS**

by

Don D. Laniewski

Thesis committee

John R. Green
Chairman

C. P. Leavitt

Victor H. Regener

378,789
Un30Lani
1961
cop. 2

TABLE OF CONTENTS

	PAGE
I. INTRODUCTION	1
II. APPARATUS	3
1. Description of Chamber	3
2. Operation	3
3. Photography	5
4. Location	6
5. Geometry of the Experiment	6
III. EXPERIMENTAL DATA	9
1. General	9
IV. DATA AND ANALYSIS	11
Part I	11
1. General	11
2. Angular Distribution as a Function of Distance From the Core	11
3. Angular Distribution of High Energy Electrons as a Function of Distance from the Core	14
Part II	21
1. General	21
2. Zenith Angle Distribution	22
3. Experimental Determination of the Zenith Angle Distribution	24
4. Comparison With Other Experiments	26

1953
K. S. ...
101

I. INTRODUCTION

II. APPARATUS

 1. Description of Apparatus

 2. Operation of Apparatus

 3. Instrumentation

 4. Location

 5. Geometry of the Experiment

III. EXPERIMENTAL RESULTS

 1. General

IV. DATA AND ANALYSIS

 Part I

 1. General

 2. Angular Distribution of a Function of

 3. Discrete Functions of

 4. Angular Distribution of

 5. Asymptotic Behavior of

 6. Error for

 Part II

 1. General

 2. Angular Distribution of

 3. Asymptotic Behavior of

 4. Comparison with

PAGE

V. ACKNOWLEDGEMENTS 28

VI. REFERENCES 29

11

12

13

14

STATE OF CALIFORNIA . V .

THE PEOPLE . V .

MILLERS FALLS

EVERETT

LIST OF TABLES AND FIGURES

TABLE	PAGE
1. Mean Projected Angle as a Function of Distance from the Core	12
2. Mean Projected Angle of High Energy Electrons as a Function of Distance from the Core	17
FIGURE	PAGE
1. Experimental Geometry	8
2. Mean Projected Angle as a Function of Distance from the Core	13
3. Mean Projected Angle of High Energy Electrons as a Function of Distance from the Core	18
4. Relation Between the Observed Projected Angle and the Space Angles	25

MILLER, F. A. L.

EXPERIMENTAL

ON THE PROJECTION OF POINTS ON A CURVE

TABLE

1. Mean projected angle as a function of distance from the core
2. Mean projected angle of 100 points
3. Mean projected angle as a function of distance from the core

FIGURE

1. Experimental geometry
2. Mean projected angle as a function of distance from the core
3. Mean projected angle of 100 points
4. Relation between the observed projected angle and the space angle

LIST OF PLATES

PLATE	PAGE
1. Cloud Chamber	4
2. Cloud Chamber and Scintillator Structure	7
3. Typical Low Energy Electrons	15
4. Typical High Energy Electrons	16
5. High Energy Electrons With Parallel Tracks	23

MILLERSVILLE STATE

- 1. Cloud Chamber
- 2. Cloud Chamber and Particle Spectrometer
- 3. Typical Low Energy Spectrometers
- 4. Typical High Energy Spectrometers
- 5. High Energy Spectrometers with Particle Tracers

I. INTRODUCTION

The earth's atmosphere is constantly being bombarded by high energy particles from outer space known as "primary cosmic rays". As they penetrate the atmosphere, these particles, which consist of protons, alpha particles and heavier nuclei, lose energy through collisions and give rise to secondary particles consisting of protons, neutrons, and both neutral and charged pi-mesons. The neutral pi-mesons almost immediately disintegrate into photons which then multiply into electromagnetic cascades. Charged pi-mesons disintegrate into mu-mesons and neutrinos. Mu-mesons interact with nuclei weakly; therefore they lose energy by ionization until they decay into electrons and neutrinos. Thus in the atmosphere one may find protons, neutrons, pi-mesons, mu-mesons, electrons, and photons.¹ Electrons are the main products of an extensive air shower and comprise approximately 90% of the shower. Since these electrons are the most numerous particles near the axis of a large shower and are easily detected, extensive air showers are most easily studied by means of the electronic component. Thus, whatever concern there may be about the nucleonic cascade of which the electron is an outgrowth, it is necessary first to understand the development of the electronic component and its lateral and angular distribution. Also, for the correct analysis of any experimental data, it is of particular importance to know something about the

angular distribution of the particles at a prescribed distance from the axis of the shower. These effects are quite often concealed because of the zenith-angle distribution. These problems are quite complicated mathematically,^{2,3} and it was the purpose of this experiment to gain some information on these problems.

Since the actual tracks left by the electronic component can be photographed and analyzed, a cloud chamber was used at the principal piece of equipment in this experiment. The results of this investigation furnished the basis of this paper. Details of the experiment, analysis of data, interpretation of results, and comparison of these results with those of other experiments and theories are treated in subsequent parts of the paper.

II. APPARATUS

1). Description of Chamber

The cloud chamber, Plate I, designed and built by John R. Green, was operated at the rear of the Physics Department of the University of New Mexico during the experiment. It is constructed of brass with the outside dimensions being 12 3/4 inches high, 12 inches wide, and 16 inches deep.⁴ The cloud chamber is a constant-pressure change type,⁵ utilizing the release of excess pressure to cool the chamber gas sufficiently to form the saturated vapor necessary to form droplets.

The chamber was operated at an expanded pressure of approximately 1.15 atmospheres of argon with sufficient alcohol to give tracks with an expansion ratio of 1.13.

The front and both sides were covered with 1/2 inch glass for viewing and observation. The center of the chamber contained 1/2 inch of lead plate.

2). Operation

The cloud chamber was used in conjunction with other experiments being performed in connection with extensive air showers. Triggering of the cloud chamber will be described in more detail later in the paper. Simply, a pulse was used to trigger a thyratron, the discharge of which was used to energize an electromagnet which in turn released an arm that normally maintained an air-tight condition between the rear

1. Description of Apparatus

The closed chamber, 10 in. diameter and 12 in. high, was constructed of stainless steel and was mounted on a base of the same material. The chamber was connected to a vacuum pump through a 1/2 in. diameter stainless steel pipe. The chamber was equipped with a viewing glass for viewing and a pressure gauge for measuring the pressure. The chamber was also equipped with a cooling coil and a condenser. The chamber was equipped with a viewing glass for viewing and a pressure gauge for measuring the pressure. The chamber was also equipped with a cooling coil and a condenser. The chamber was equipped with a viewing glass for viewing and a pressure gauge for measuring the pressure. The chamber was also equipped with a cooling coil and a condenser.

2. Operation

The closed chamber was operated at a pressure of approximately 100 mm. Hg. The chamber was equipped with a viewing glass for viewing and a pressure gauge for measuring the pressure. The chamber was also equipped with a cooling coil and a condenser. The chamber was equipped with a viewing glass for viewing and a pressure gauge for measuring the pressure. The chamber was also equipped with a cooling coil and a condenser.

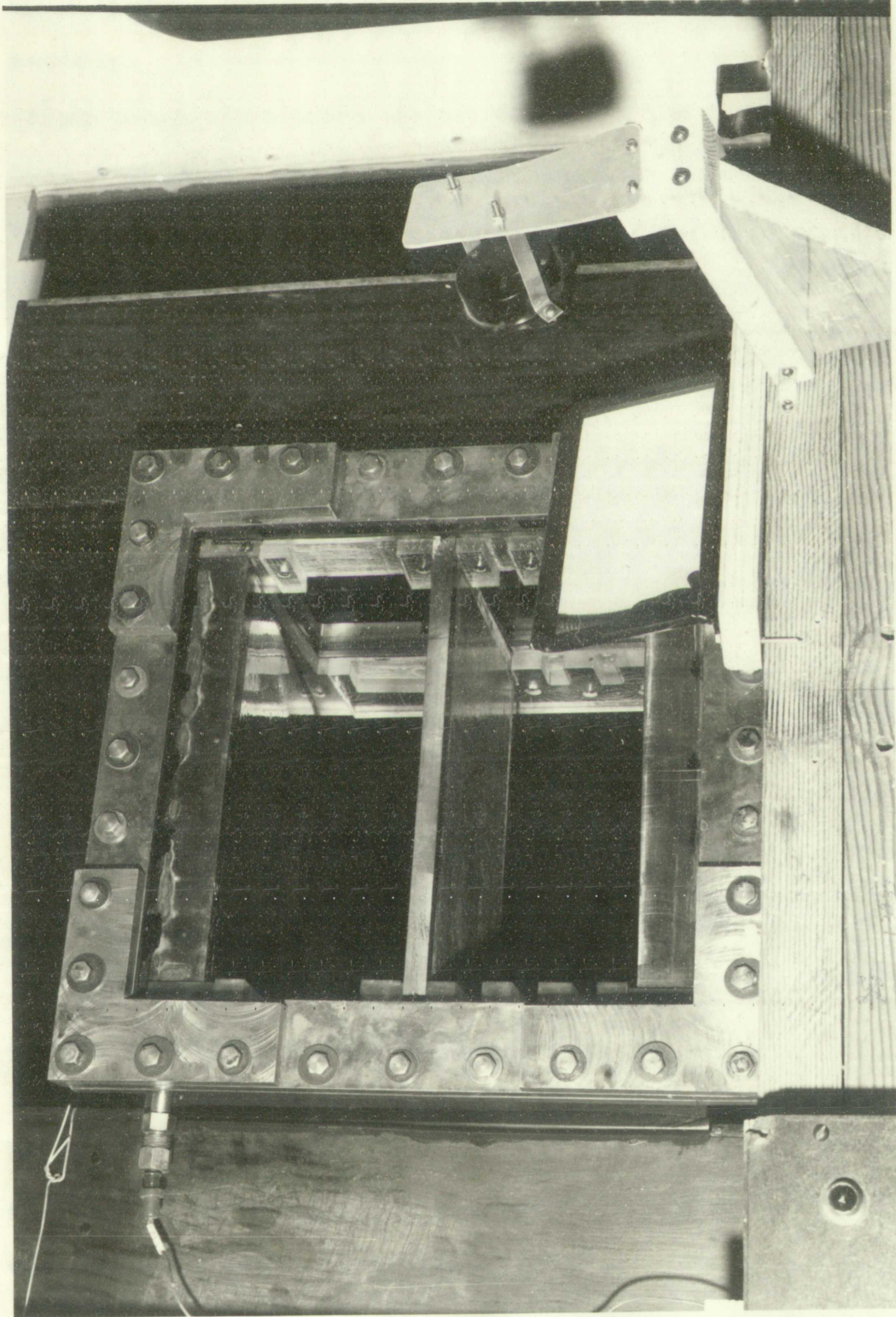


Plate 1.



trap door and a rubber gasket. Greater detail can be obtained in Reference 4. The chamber was then allowed to expand rapidly. After the expansion had taken place, and a photograph taken, the chamber was reset automatically for the next expansion. This resetting was operated by a motor which was started by the expansion. The operations that followed were simply:

- 1). The arm of the magnet was brought back into position.
- 2). The chamber was expanded twice at a very slow rate. Such slow expansions were utilized for clearing the chamber of small droplets that did not evaporate readily.
- 3). The film of the photographing camera was advanced.

During the recycling of the chamber, the chamber was insensitive to rapid expansions. This period lasted approximately two minutes.

3). Photography

The chamber was photographed by means of a stereoscopic camera placed four feet from the front of the chamber. To eliminate the need for fast shutter synchronization, the camera had no shutter and was open constantly; therefore it was necessary to keep the camera and chamber in a dark enclosure by means of a "cloth-tent".

The film used was Kodak Linograph Ortho 35 mm. film

trap door and a rubber gasket. The chamber was then allowed to expand rapidly. After the expansion had taken place, the chamber was cooled to the next expansion. This procedure was repeated until the expansion which was caused by the expansion. The other expansions followed were similar.

- 1) The aim of the experiment was to determine the position.
- 2) The chamber was expanded until it reached a certain rate. Each time expansion was reached, the chamber was cooled to the next expansion. This procedure was repeated until the expansion which was caused by the expansion. The other expansions followed were similar.
- 3) The aim of the experiment was to determine the position. During the cooling of the chamber, the chamber was expanded to the next expansion. This procedure was repeated until the expansion which was caused by the expansion. The other expansions followed were similar.

3) Photography

The chamber was photographed by means of a camera. The camera was placed four feet from the chamber. To eliminate the need for fast shutter speed, the camera had no shutter and was kept continuously open. It was necessary to keep the shutter and camera in a dark enclosure by means of a light-tight enclosure. The film used was Kodak Ektachrome.

STATION COMPANY

and was processed normally. Illumination was provided by photoflash tubes at both sides of the chamber.

4). Location

The cloud chamber was operated at the rear of the Physics Department at the University of New Mexico, Albuquerque, New Mexico (elevation 1575 meters). It was situated approximately 8 feet from the main scintillator tank and housed in a building attached to the scintillator structure. See Plate II. The roof of the housing was made of 3/4 inch exterior plywood. The housing was kept at a constant temperature (approximately $23 \pm 2^{\circ}\text{C}.$) by sufficient insulation and the use of heaters and a refrigeration unit.

5). Geometry of the Experiment

The experimental set-up consisted of five liquid scintillation detectors. Two of the scintillators that are 10 feet in diameter are placed to form a vertical telescope. The same structure that housed these scintillators also housed the cloud chamber as discussed earlier. The three other scintillators are three feet in diameter and are arranged in the form of an isosceles triangle with the larger scintillators. Figure 1 shows the arrangement.

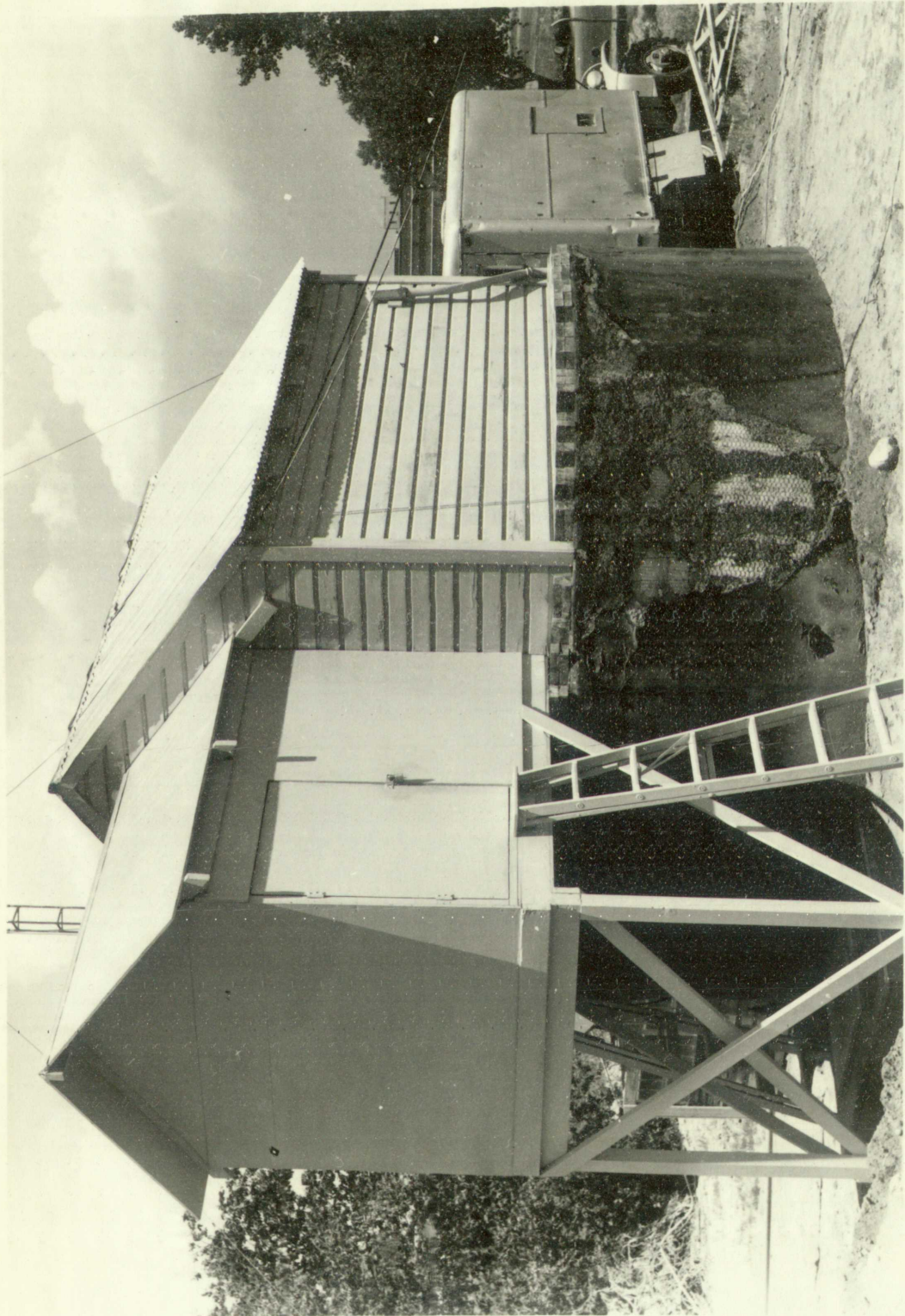
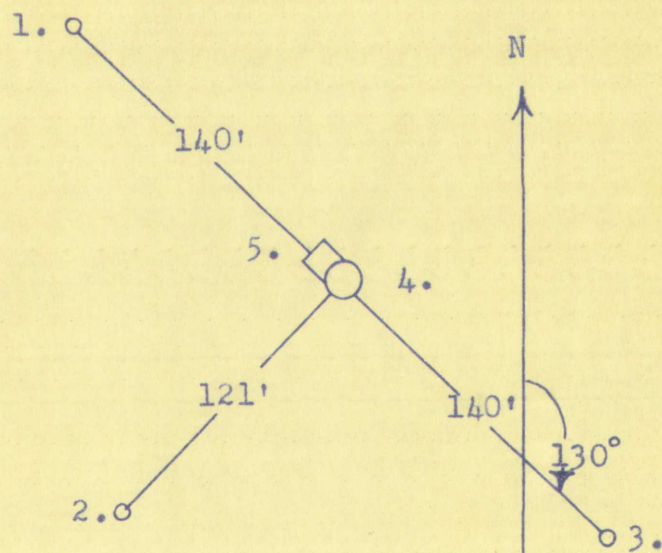


Plate 2.

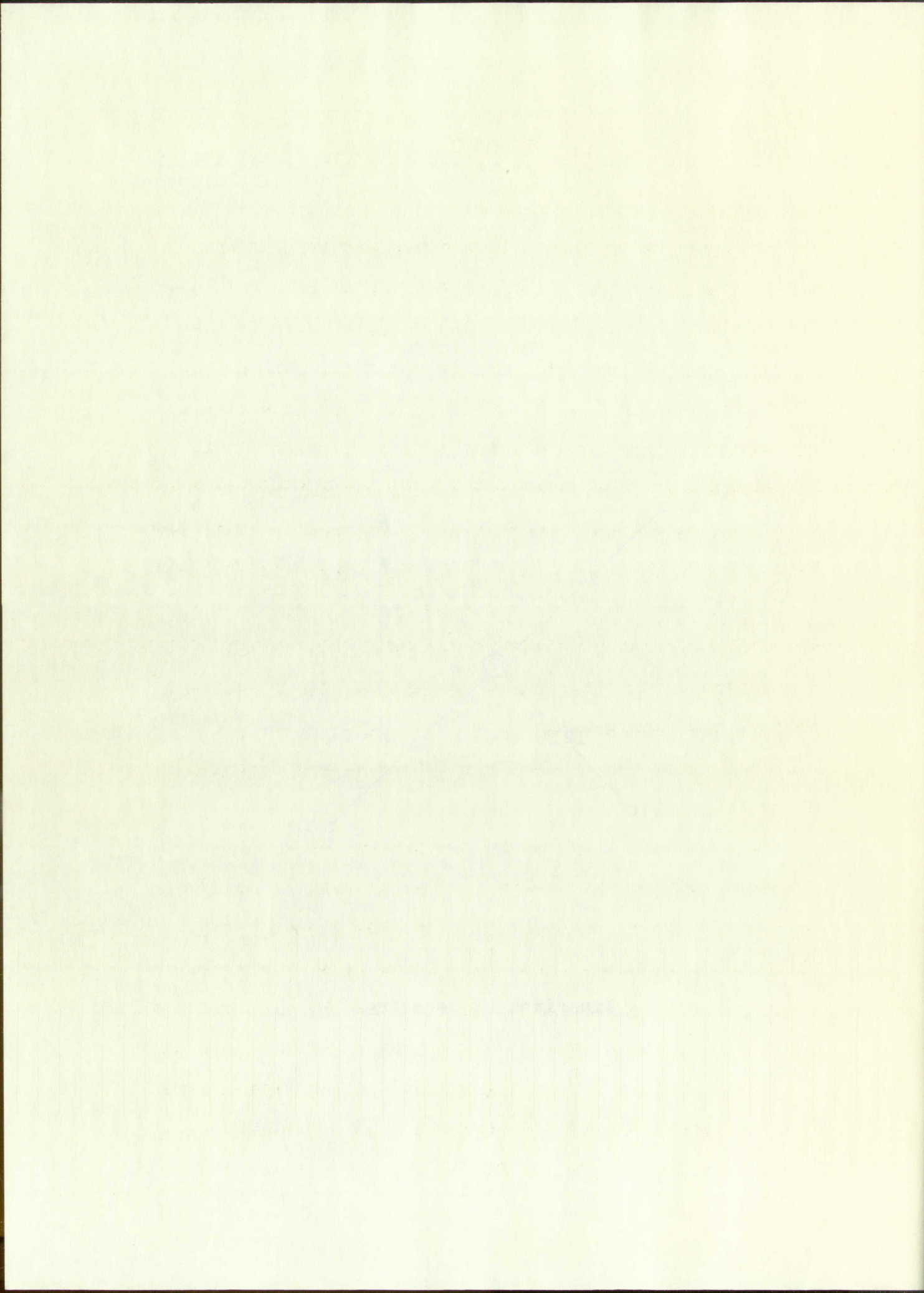


- 1, 2, and 3. 3-ft. Scintillators
4. Vertical Telescope
5. Cloud Chamber



Experimental Geometry

Fig. 1



III. EXPERIMENTAL DATA

1). General

Triggering of the cloud chamber was accomplished by means of pulses from the upper scintillator of the vertical telescope. The output pulse was discriminated so that a triggering pulse was supplied to the cloud chamber only when the particle density was greater than approximately 100 particles per square meter at the location of the large scintillator. This corresponds to a minimum shower size of approximately 4×10^4 particles.⁶ The minimum size for which the entire array, including the three smaller scintillators, was sensitive was 6×10^5 particles. Therefore, the events selected by the single scintillator are representative, on the average, of a smaller size shower than that of the main array.

Each time the chamber was triggered and expanded, a photograph of the event was taken.

At the same time, as an independent experiment by another student, the density of the shower, as observed in each of the scintillating tanks, was automatically recorded by an I.B.M. machine. These data furnished the basis for the determination of the core location and size of the shower. The author of this paper utilized these core locations in part of the analysis of his own experiment.

Of approximately four hundred pictures taken, only sixty were found to be useful in the part of the experiment

1) General

Triggering of the cloud chamber was accomplished by means of pulses from the output of a photomultiplier telescope. The central part of the telescope was triggered by a pulse from the output of a photomultiplier when the particle detector was triggered. This corresponds to a pulse from the output of a photomultiplier of approximately 400 e.v. The entire system, including the photomultiplier, was mounted on a base which was selected by the trigger. The events selected by the trigger were analyzed in detail on the average of the events. That of the data were.

Each time the shower was triggered and a photograph of the event was taken. At the same time, as an independent check, another shower, the energy of the shower was observed in each of the coincident channels, and the results recorded by an electronic counter. These data were used as a check for the calibration of the counter. The shower, the energy of the shower was observed in each of the coincident channels in part of the analysis of the data. Of approximately 1000 showers were recorded. Sixty were found to be caused by the trigger.

having to do with core locations. A large percentage of the unused pictures consisted of showers for which it was not possible to determine the location of the core. This was brought about by the fact that the tanks that determined the location of the core were not run in four-fold coincidence with the scintillator that controlled the cloud chamber. Most of the unusable pictures were due to periods of operation of an improperly expanded chamber.

REPORT OF THE

having to do with the...
unusual...
possible to determine...
brought about...
the location of the...
with the...
Most of the...
tion of an...

IV. DATA AND ANALYSIS

Part I

1). General

After the film was processed, those events for which the entire array was sensitive were sorted out. Enlargements were made on 8x10 inch projection paper and then analyzed. The following data were extracted from the enlargements:

- 1). The angles measured on the enlargements between the zenith and the direction of the incident particle in the upper half of the chamber. Measurements were not made in the lower portion of the chamber because of the scattering in the lead.
- 2). The same angles measured as in 1)., but only for those incident particles for which a minimum multiplicity of three could be observed below the $\frac{1}{2}$ inch of lead.
- 3). The general direction of the particles, that is, whether they appeared to be incident from the left or right side of the chamber.

2). Angular Distribution as a Function of Distance from the Core.

The angles measured from the vertical for all the incident particles were summed and averaged for each event.

These averaged angles were plotted as a function of distance from the point of impact of the shower. The results are shown in the following table and graphically in Figure 2.

R (feet)	θ (degrees)	R (feet)	θ (degrees)
12	17.4	61	20.9
16	24.2	62	19.5
19	18.6	73	15.8
20	22.7	74	25.3
22	12.5	75	8.4
23	15.4	75	12.7
25	21.1	82	15.2
30	22.9	82	27.0
32	15.0	87	21.5
37	16.5	88	18.9
42	30.1	93	27.3
43	23.6	95	31.2
45	15.4	97	19.4
45	22.8	100	21.3
47	13.4	100	25.2
49	20.8	106	13.1
53	20.8	115	15.8
54	22.5	115	12.0
55	12.0	130	17.5
59	16.7	140	11.1
61	22.6	140	19.2

Calculations by Galbraith⁷ show that the scattering angle of electrons is inversely proportional to the total energy of the electrons; that is, the highest energy particles are least scattered and are found nearest the core. As seen from the graph in Figure 2, however, the observed average projected angle is not a function of the distance from the core. In fact, there appears to be no correlation between the distance and the angles measured.

These curves are also shown in Figure 1. The curves are plotted from the point of intersection of the curves with the vertical axis shown in the following table and are drawn by hand.

R (feet)	C (the curve)	D (the curve)
12	1.00	1.00
13	1.00	1.00
14	1.00	1.00
15	1.00	1.00
16	1.00	1.00
17	1.00	1.00
18	1.00	1.00
19	1.00	1.00
20	1.00	1.00
21	1.00	1.00
22	1.00	1.00
23	1.00	1.00
24	1.00	1.00
25	1.00	1.00
26	1.00	1.00
27	1.00	1.00
28	1.00	1.00
29	1.00	1.00
30	1.00	1.00
31	1.00	1.00
32	1.00	1.00
33	1.00	1.00
34	1.00	1.00
35	1.00	1.00
36	1.00	1.00
37	1.00	1.00
38	1.00	1.00
39	1.00	1.00
40	1.00	1.00
41	1.00	1.00
42	1.00	1.00
43	1.00	1.00
44	1.00	1.00
45	1.00	1.00
46	1.00	1.00
47	1.00	1.00
48	1.00	1.00
49	1.00	1.00
50	1.00	1.00
51	1.00	1.00
52	1.00	1.00
53	1.00	1.00
54	1.00	1.00
55	1.00	1.00
56	1.00	1.00
57	1.00	1.00
58	1.00	1.00
59	1.00	1.00
60	1.00	1.00

Calculations by hand were made for the angle of elevation of the electron at various points along the path. The energy of the electron at the point of emission was assumed to be 100 e.v. and the energy at the point of absorption was assumed to be 10 e.v. The average velocity was assumed to be 100,000 m.p.s. The distance between the plates was assumed to be 1 cm. The results are shown in the following table.

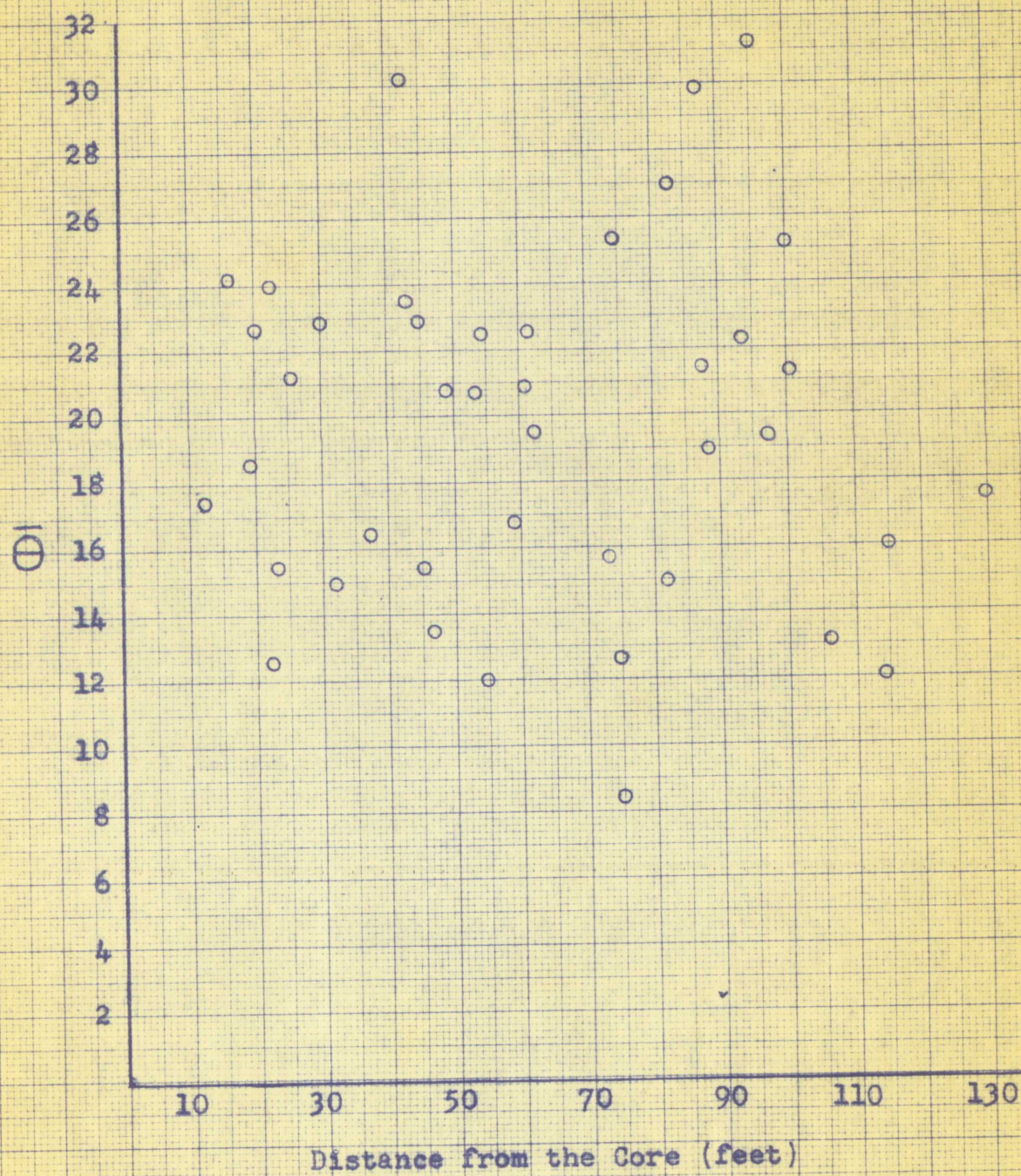
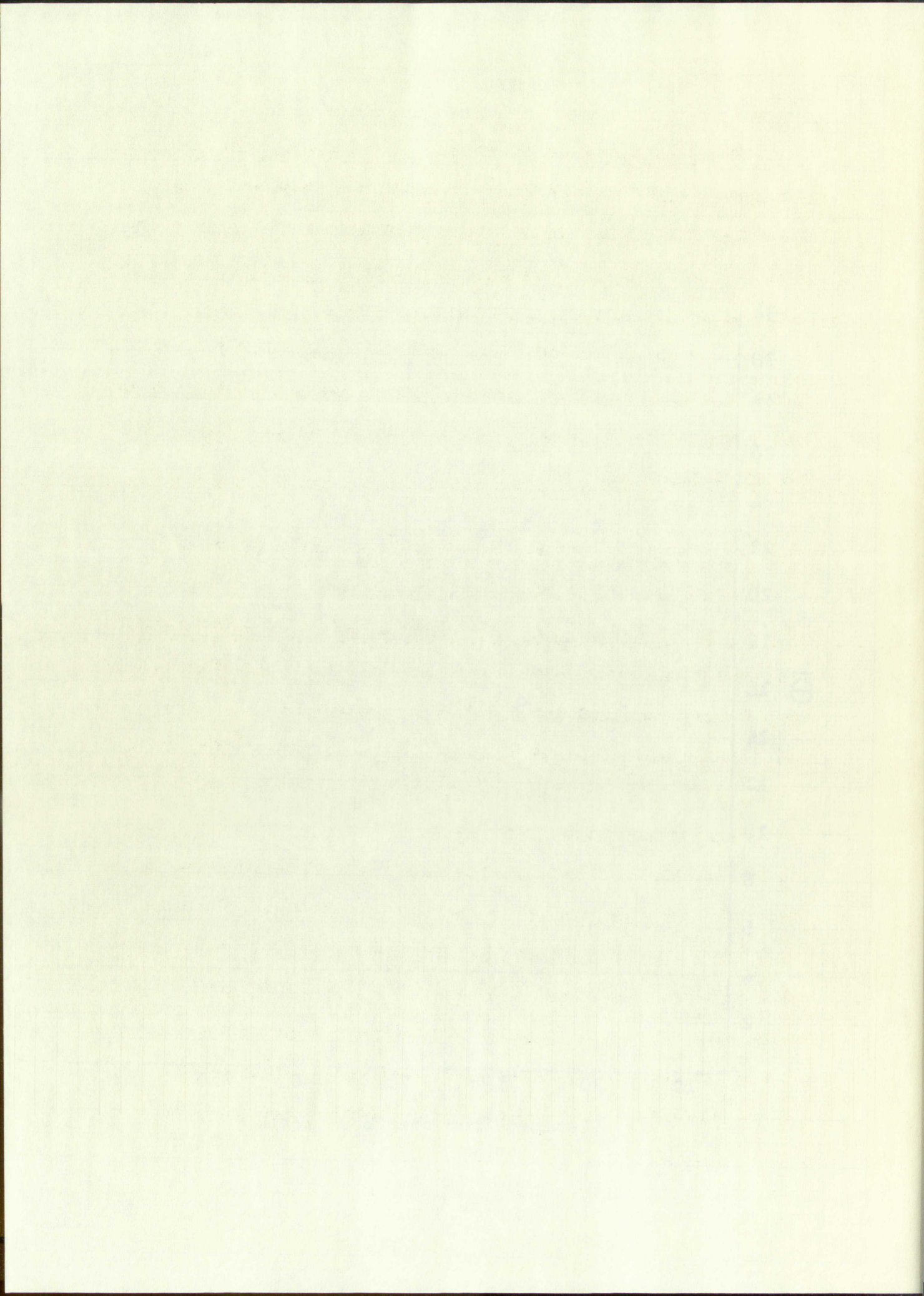


Fig. 2



According to calculations of Roberg and Nordheim,⁸ low energy electrons diffuse in random directions. Their spectrum show about 1/6 of all electrons in the shower are composed of these low energy electrons. An example of such low energy electrons can be seen in Plate III. Since such low energy particles were included in obtaining the results shown in Figure 2, the distribution seems to indicate that low energy electrons are of considerable importance at all radial distances.

3). Angular Distribution of High Energy Electrons as a Function of Distance From the Core.

To find the angular distribution of higher energy electrons, the photographs were re-analyzed, and only those tracks that resulted in a minimum multiplicity of three particles upon interaction with a $\frac{1}{2}$ inch lead plate in the center of the chamber were considered. This was done to set some criterion for the energy of the incident particles for which the angular distributions would be determined. From the calculations of Ivanenko,⁹ such a multiplicity would require the initiating particle to have a minimum energy of approximately 165 Mev. Typical of these is the event shown in Plate IV. As was done previously, the projected angles were measured and averaged, and were plotted as a function of the distance of impact of the shower.

According to calculations of the energy spectrum of low energy electrons, the spectrum shows a peak at 1.5 eV, which is composed of two low energy peaks. The low energy peaks are shown in Figure 2. The distance between the two low energy peaks is 0.5 eV. The distance between the two low energy peaks is 0.5 eV.

3) Another Example of the Energy Spectrum
Function of the Energy Spectrum

To find the energy spectrum of the electrons, the spectrum was calculated, and the results are shown in Figure 3. The spectrum shows a peak at 1.5 eV, which is composed of two low energy peaks. The low energy peaks are shown in Figure 4. The distance between the two low energy peaks is 0.5 eV. The distance between the two low energy peaks is 0.5 eV.

COLLISION CONTROL
EXPERIMENT

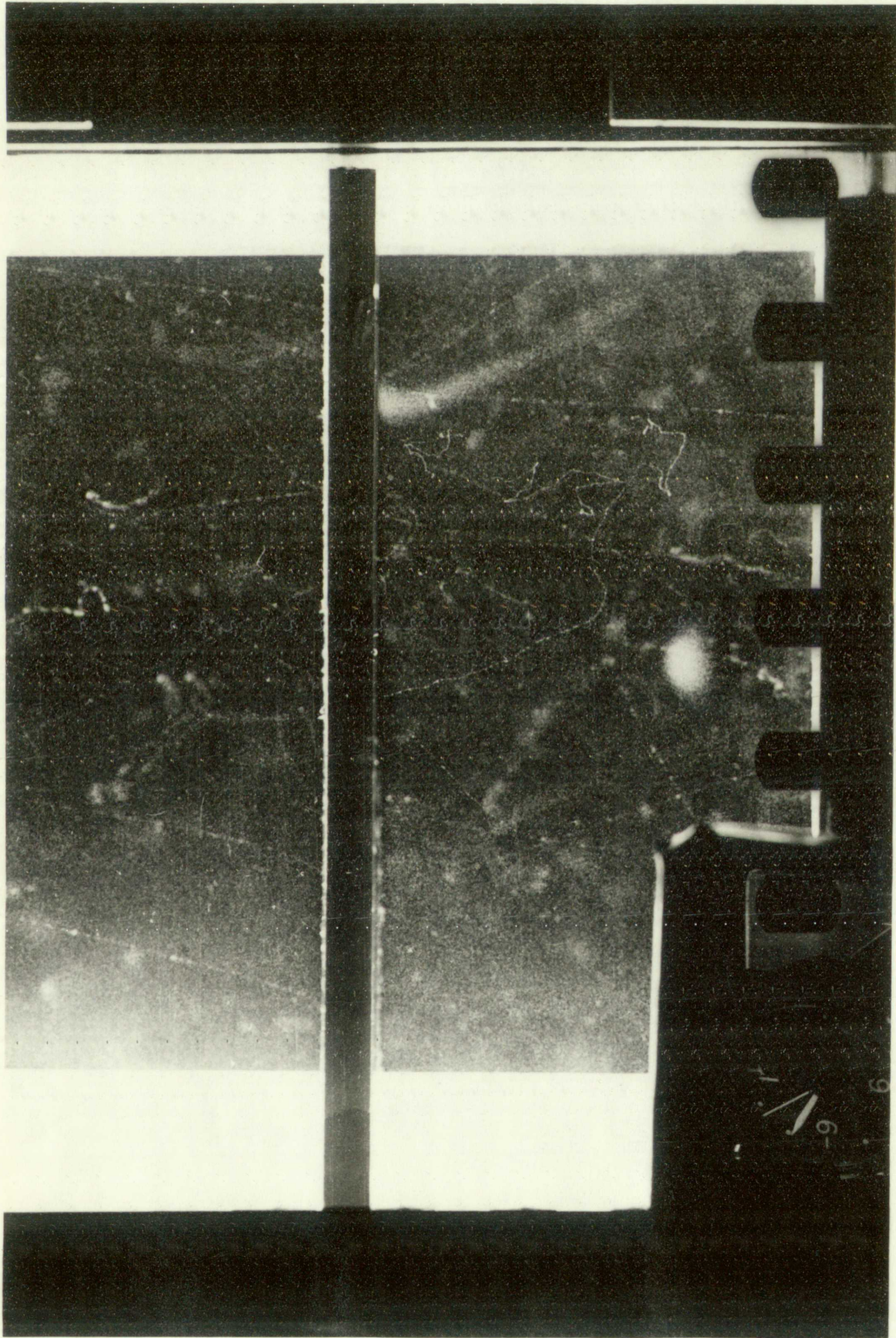


Plate 3.



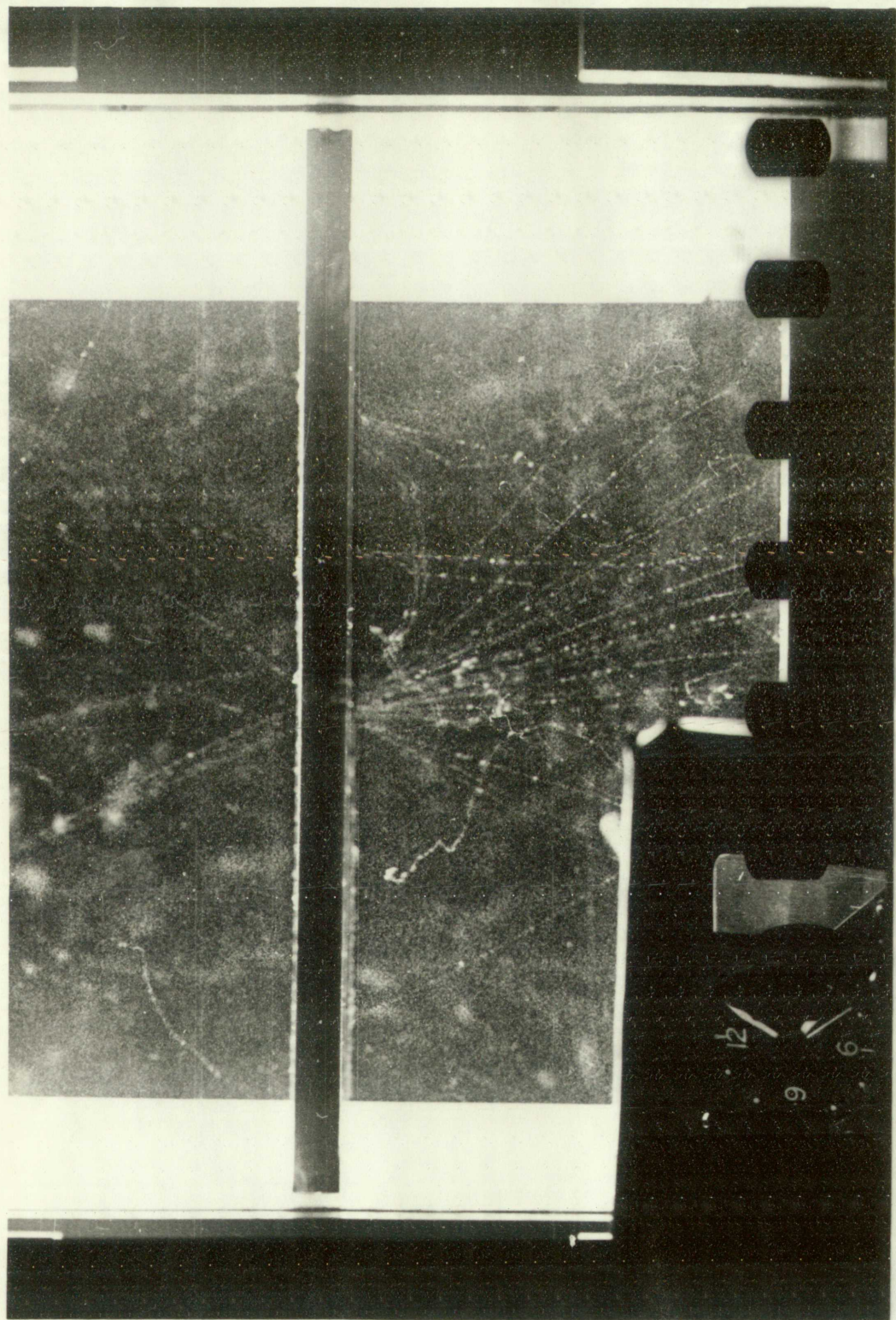


Plate 4.



The distribution is shown in the following table and graphically in Figure 3.

R (feet)	$\bar{\theta}$ (degrees)	R (feet)	$\bar{\theta}$ (degrees)
12	14.3	61	15.0
16	24.0	62	16.0
22	9.3	75	2.0
22	10.0	82	6.0
25	12.7	82	25.0
30	5.0	88	22.5
32	11.0	93	3.0
42	26.0	97	12.5
45	3.0	100	4.5
45	20.6	100	4.0
47	10.3	106	14.0
49	11.2	115	3.5
53	11.6	140	3.6

Even though the low energy electrons (which would have given large angle scattering) were eliminated, the mean angle distribution is still found to be poorly correlated with the distance from the shower. As is evident from the graph, however, the average mean angle has dropped considerably.

Ivanenko showed a definite increase in the mean scattering angle as a function of distance from the core. Comparison with his results, however, would require the mean projected angle from the core direction as a function of the energy of the particles at a given distance from the core of the shower. The core direction could not be included in the analysis by the author since this determination

The distribution is shown in the following table and graph. The distribution is shown in Figure 3.

Energy (keV)	Count	\bar{E} (keV)	R (keV)
1.0	10	1.0	0.0
2.0	20	2.0	0.0
3.0	30	3.0	0.0
4.0	40	4.0	0.0
5.0	50	5.0	0.0
6.0	60	6.0	0.0
7.0	70	7.0	0.0
8.0	80	8.0	0.0
9.0	90	9.0	0.0
10.0	100	10.0	0.0
11.0	110	11.0	0.0
12.0	120	12.0	0.0
13.0	130	13.0	0.0
14.0	140	14.0	0.0
15.0	150	15.0	0.0
16.0	160	16.0	0.0
17.0	170	17.0	0.0
18.0	180	18.0	0.0
19.0	190	19.0	0.0
20.0	200	20.0	0.0

Even though the low energy electrons have given large angle scattering, the angle distribution is still broad in the energy range with the distance from the source. In the graph, however, the energy range has been expanded.

Investigation showed a definite increase in the scattering angle as a function of distance from the source. Comparison with the theoretical distribution with the mean projected angle shows that the angle of the energy at the center of the source is included in the results. The angle of the energy at the center of the source is included in the results of the graph.

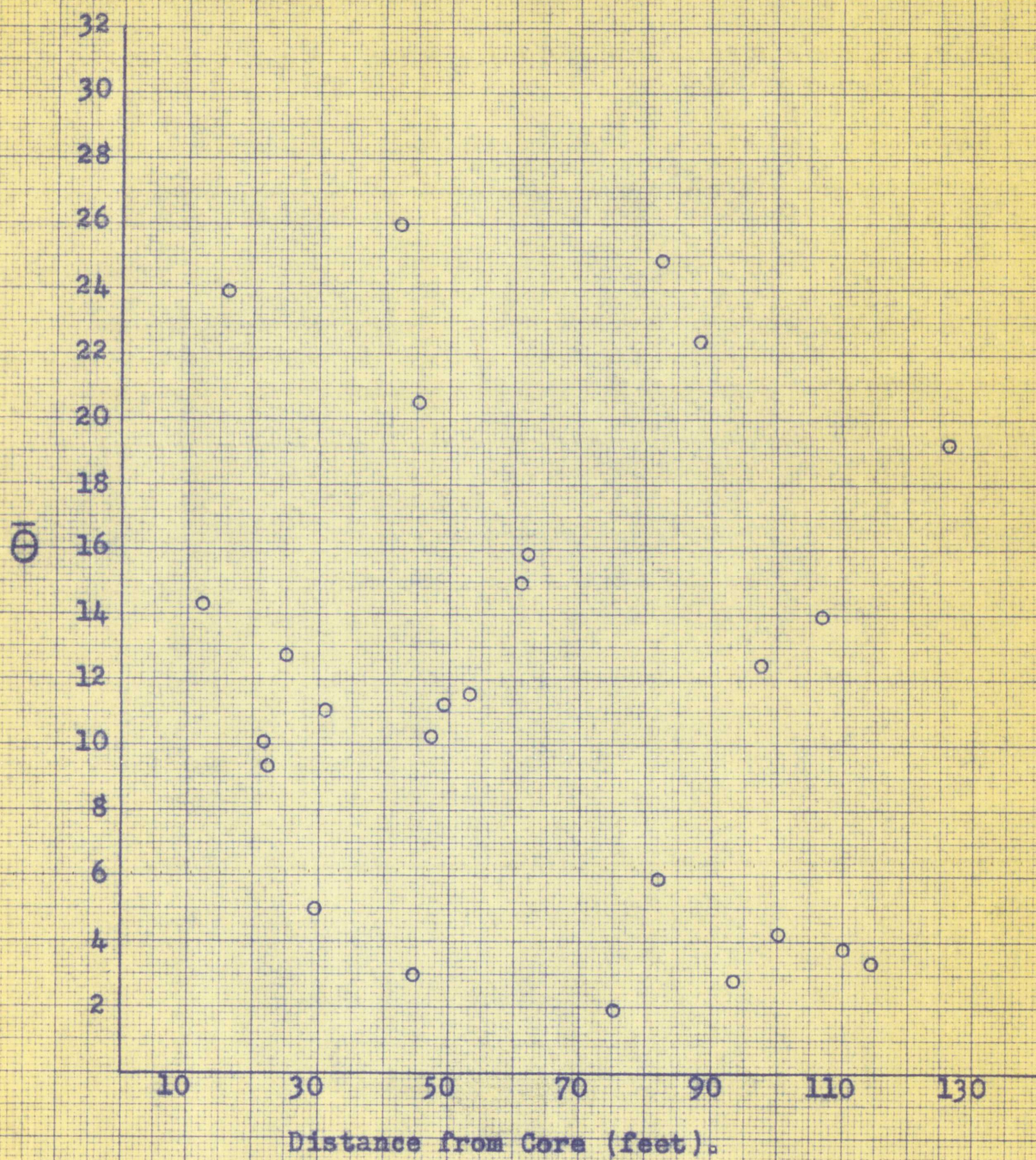


Fig. 3

was not possible with the experimental set-up. Since the results in Figure 3 do not show the distribution as predicted by Ivanenko, it was deemed necessary to investigate the situation further.

A distribution was made utilizing the same values of $\bar{\theta}$ and the core distance but also utilizing the direction of the core as observed from the photographs. The photographs of the incident particles were classified as either positive or negative, depending upon whether the particles appeared to arrive from the northern or southern directions respectively. Because of the location of the camera and two-dimensional photography, it was impossible to determine which showers arrived from the east-west directions. Reference was made to the azimuth angle of the point of impact of the shower to investigate the possible influence of the showers arriving with large angles to the zenith. The results are shown in the following table.

ϕ	No. of Particles with Azimuth Angles 0 to 180°	No. of Particles with Azimuth Angles 180 to 360°
Positive	3	5
Negative	9	9

If all the showers arrive from the zenith, then those photographs classified as positive should correspond to cores

was not possible with the experimental arrangement. The results in figure 2 do not agree with those obtained by Iversen, 1954, but the general character of the distribution is similar. A distribution was also obtained for the case of \bar{e} and the core distance but also with the distribution of the core as observed from the photographs. The distribution of the incident particles was also studied in other studies or negative, depending upon whether the vertical distance to arrive from the horizontal or vertical distance respectively. Because of the location of the camera and the dimensional photography, it was impossible to determine which showers arrived from the east-west direction. Reference was made to the relative angle of the shower axis of the shower to the vertical and also to the relative impact of the shower to the vertical and also to the relative of the showers arriving from the east-west direction. The results are shown in the following table.

TABLE I

Relative angle of shower axis to vertical	Relative impact of shower to vertical	ϕ
Positive	Positive	Positive
Negative	Negative	Negative

If all the showers arrived from the east-west direction, the photographs of arrival at positive relative distance to core

whose locations were characterized by the azimuth angles 0 to 180° . Similarly, all photographs classified negative would have core locations characterized by azimuth angles 180 to 360° . Obviously, one can see from the table that this is not the case. The fraction of showers arriving with appreciable zenith angles is certainly not negligible. The large number of events in the negative direction can be attributed to the geometry of the experiment which favored showers whose cores fell on that side. It is apparent from the distribution that the observed angular distributions are strongly influenced by the zenith angle distribution.

The results of this analysis make it apparent that one cannot determine the angular distribution of the particles with regard to the direction of the shower axis as a function of the distance from the axis of the shower without a simultaneous knowledge of the zenith angle.

Because of the large influence of the zenith angle distribution on the observed results, it was determined to analyze the data to determine an approximate zenith angle distribution for the shower axis.

whose locations were determined by the...
to 130°. Similarly, the...
would have some locations...
100 to 300°....
this is not the case...
appreciable...
large number of events...
attributed to the...
showed those cores...
the distribution...
strongly influenced...
The result...
cannot determine...
with regard to...
of the distance...
simultaneous...
Because of the...
distribution...
analyze the data...
distribution for...

Part II

1). General

The change of shower counting rate with varying altitude, varying barometric pressure at a fixed elevation, and varying zenith angle are closely related since they all result primarily from the growth and decay of the electronic cascades as they traverse increasing amounts of matter. Interest in these phenomena persists because the development of extensive air showers is influenced not only by the properties of pure electronic cascades, but also by the shape of the primary cosmic ray energy spectrum and the nature of the process by which the primary energy is transferred to the soft component, both at the origin of the shower and throughout the associated nuclear cascade. For this paper we will be concerned with the zenith angle distribution.

There are several methods of measuring the zenith angle distribution. One method of measuring the distribution is to compare the coincidence rates obtained with counters whose axes are vertical and horizontal.¹⁰ A newly developed method is to measure the difference in time of response of counters that are separated from each other in a horizontal plane.¹¹ This method can yield the space angle distribution as well as the distribution of projected angles. An analogous method is to measure the angles of the tracks of all shower particles seen in a cloud chamber.¹² These experiments are undesirable since they yield the angular distribution,

1). General

The change of shower count rate with zenith angle, varying parabolic decrease of shower rate with increasing zenith angle are closely related since they are primarily from the geometry and theory of particle cascade processes as they traverse increasing amounts of matter. In fact, these phenomena result from the development of secondary air showers as indicated by the theory of particle cascade electronic cascades, and the fact that the rate of cosmic ray energy absorption is a function of the amount of matter which the primary energy is required to traverse, both at the origin of the shower and throughout the shower. The shower rate will be proportional to the square of the shower rate with the zenith angle distribution.

There are several methods of determining the zenith angle distribution. The method of least squares is used to compare the coincidence rate obtained with counters whose axes are vertical and horizontal. The method is to measure the difference in count rate between the two counters that are separated horizontally in a vertical plane.

II

This method can yield the zenith angle distribution as well as the distribution of shower rates. In some cases method is to measure the rate of the shower rate. Shower particles seen in a shower shower. These particles are undetectable since they are not in the detector.

not of the shower axis, but of the shower particles, many of which have been badly scattered. The method employed for this paper was to consider only those cloud chamber pictures that showed high energy electrons of nearly parallel tracks of which the average direction could be well determined. Since information in coincidence from all five tanks is no longer required, all photographs obtained were now analyzed. It is known that the response of a single scintillator, such as triggered the chamber, favors showers whose cores strike close to the apparatus,¹³ the average distance being approximately fifteen to twenty meters. At this distance from the core the average energy of the particles is still several hundred Mev. and the angular deviation from the core direction only a few degrees. Thus, this method should result in a fair approximation to the zenith angle distribution and should not be strongly influenced by the angular deviation of the particles from the direction of the axis of the shower. A typical event used is shown in Plate V.

2). Zenith-Angle Distribution

Let us assume that the zenith-angle distribution takes the form 14)

$$N(\Omega)d\Omega = A \cos^n \theta \sin \theta \, d\theta \, d\phi \quad (1)$$

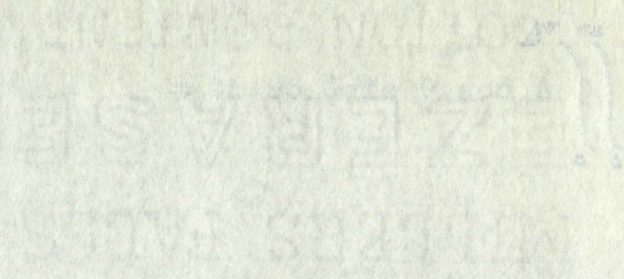
where A is the normalizing constant equal to $\frac{n+1}{2\pi}$, so that

$$\int_0^{2\pi} \int_0^{\pi/2} A \cos^n \theta \sin \theta \, d\theta \, d\phi = 1 \quad (2)$$

not of the answer... which have been... this paper was... that showed... of which the... Since information... longer received... It is known... as explained... close to the... nearly fifteen... core the average... hundred feet... only a few... fair approximation... not be strongly... particles from... typical events...

2. Smith-Angle Distribution

Let us assume that the... the form (1)... where A is the... that



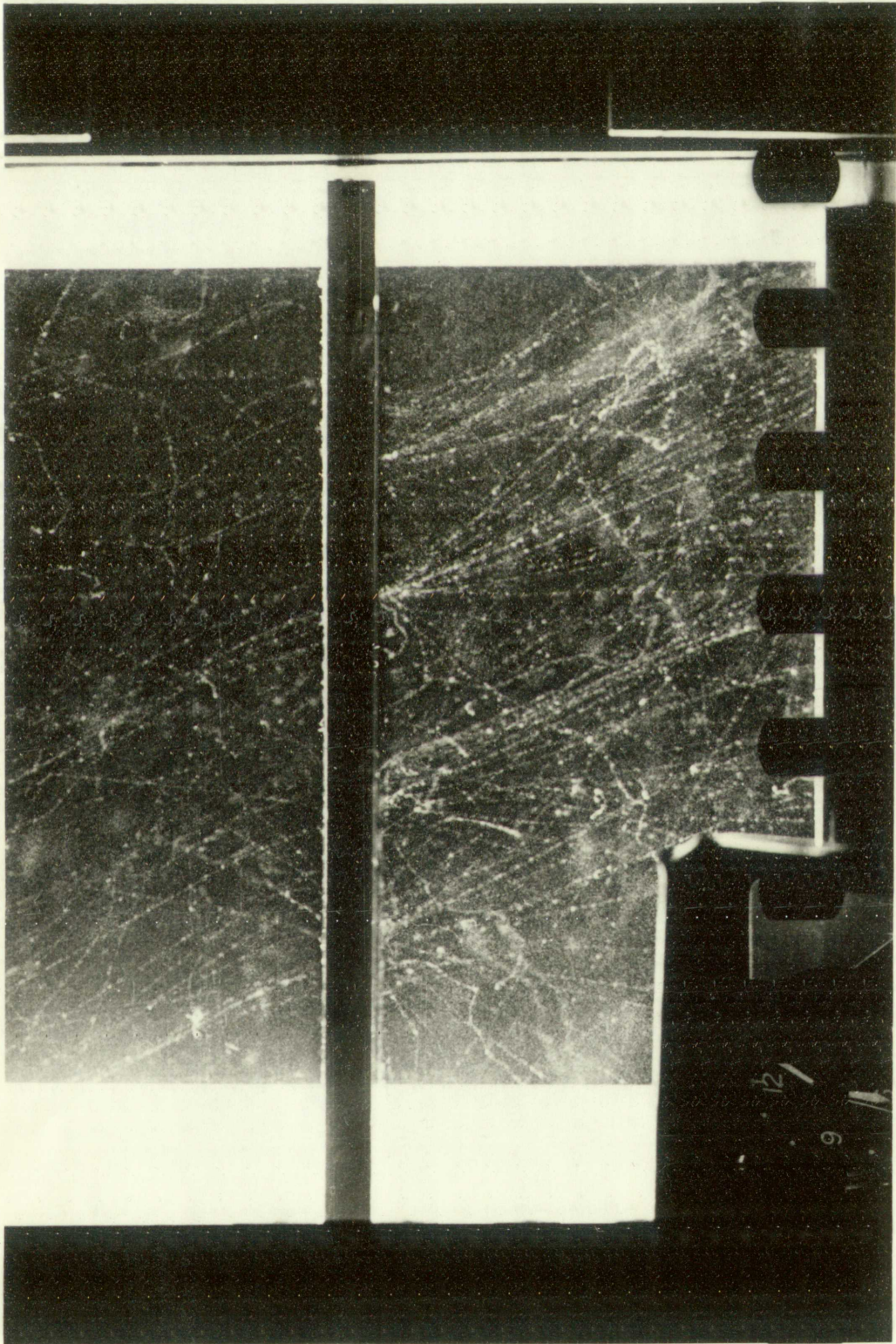
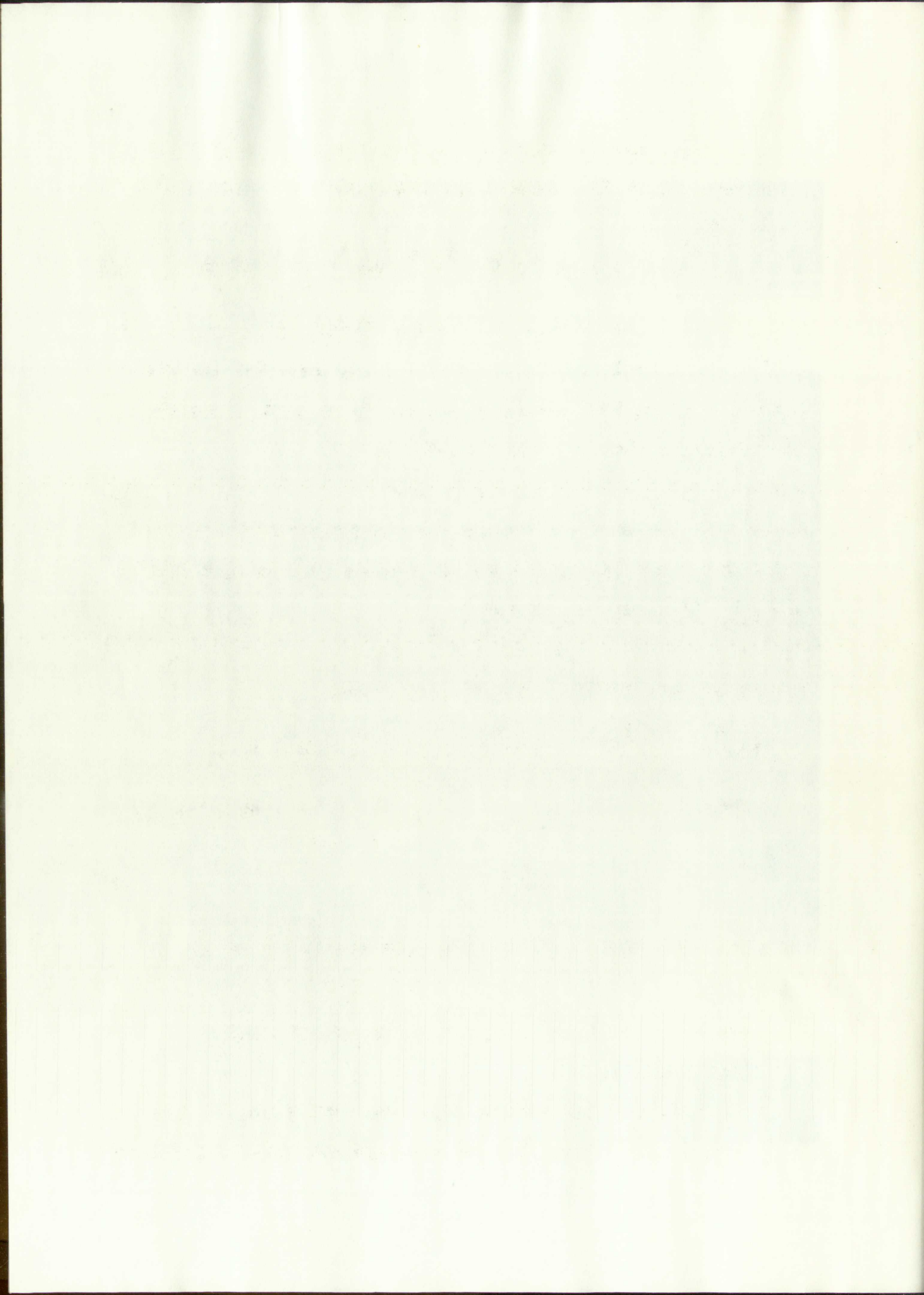


Plate 5.



This zenith angle distribution gives the probability per unit solid angle for showers arriving at the zenith angle θ . Therefore

$$P(\theta, \phi) \sin \theta \, d\theta \, d\phi = \frac{n+1}{2\pi} \cos^n \theta \sin \theta \, d\theta \, d\phi \quad (3)$$

Since these distributions are computed for space-angle distributions, a relationship must be developed for the distribution of projected angles which are used in this paper.

From Figure 4 the relation is seen to be

$$\tan \theta_p = \tan \theta \cos \phi \quad (4)$$

where θ_p is the projected angle on the plane of observation and θ and ϕ are the space zenith and azimuth angles respectively. Squaring, we obtain

$$\tan^2 \theta_p = \tan^2 \theta \cos^2 \phi$$

Inserting this in the integral, we obtain

$$\tan^2 \theta_p = \int_0^{\pi/2} \int_0^{2\pi} \frac{n+1}{2\pi} \cos^n \theta \sin \theta \tan^2 \theta \cos^2 \phi \, d\theta \, d\phi$$

The integral can be evaluated in a straightforward manner to give

$$\tan^2 \theta_p = \frac{1}{n-1} \quad (5)$$

From the above function, we can find the value of n .

3). Experimental Determination of the Zenith Angle Distribution.

To determine the zenith angle distribution, it was necessary to review all of the photographs taken during the

This result can be obtained by projecting the unit solid angle for the given angle θ onto the plane of projection. Therefore

$$P(\theta) = \frac{1}{4\pi} \int_{\Omega} \cos^2 \theta \, d\Omega \quad (1)$$

Since these distributions are projected on the plane of projection, a relationship will be derived between the distribution of projected angles and the distribution of angles.

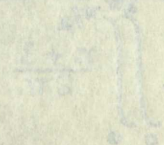
From Figure 1 the relation is seen to be

$$\cos \theta = \frac{r}{R}$$

where θ is the projected angle and r is the radius of the projection. and θ and r are the angles and radii respectively.

$$\frac{d\Omega}{\sin \theta} = \frac{2\pi r \, dr}{R^2} \quad (2)$$

Inserting this in the integral, we obtain

$$\tan \theta = \frac{r}{z} = \frac{R \sin \theta}{R \cos \theta} = \tan \theta$$


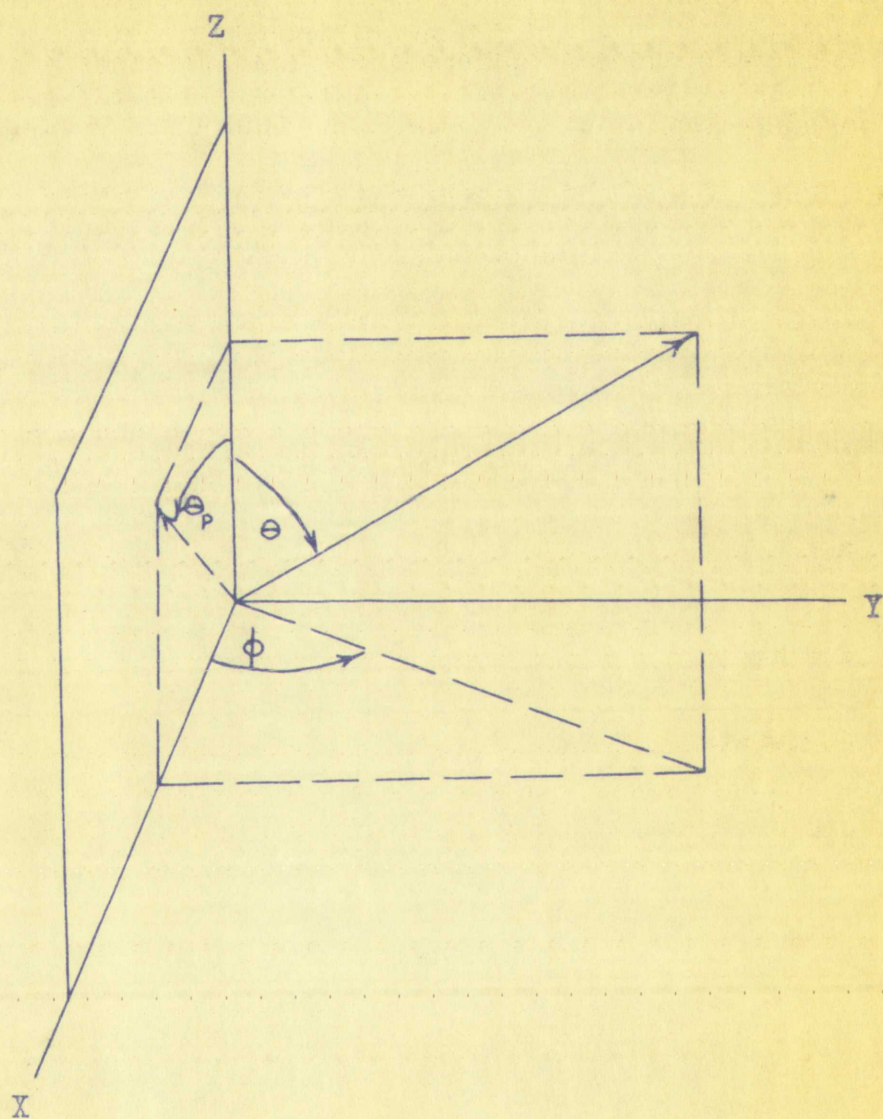
The integral can be evaluated as follows:

$$\int_0^{\pi/2} \cos^2 \theta \sin \theta \, d\theta = \frac{1}{3} \sin^3 \theta \Big|_0^{\pi/2} = \frac{1}{3}$$

From the above derivation, we can see that

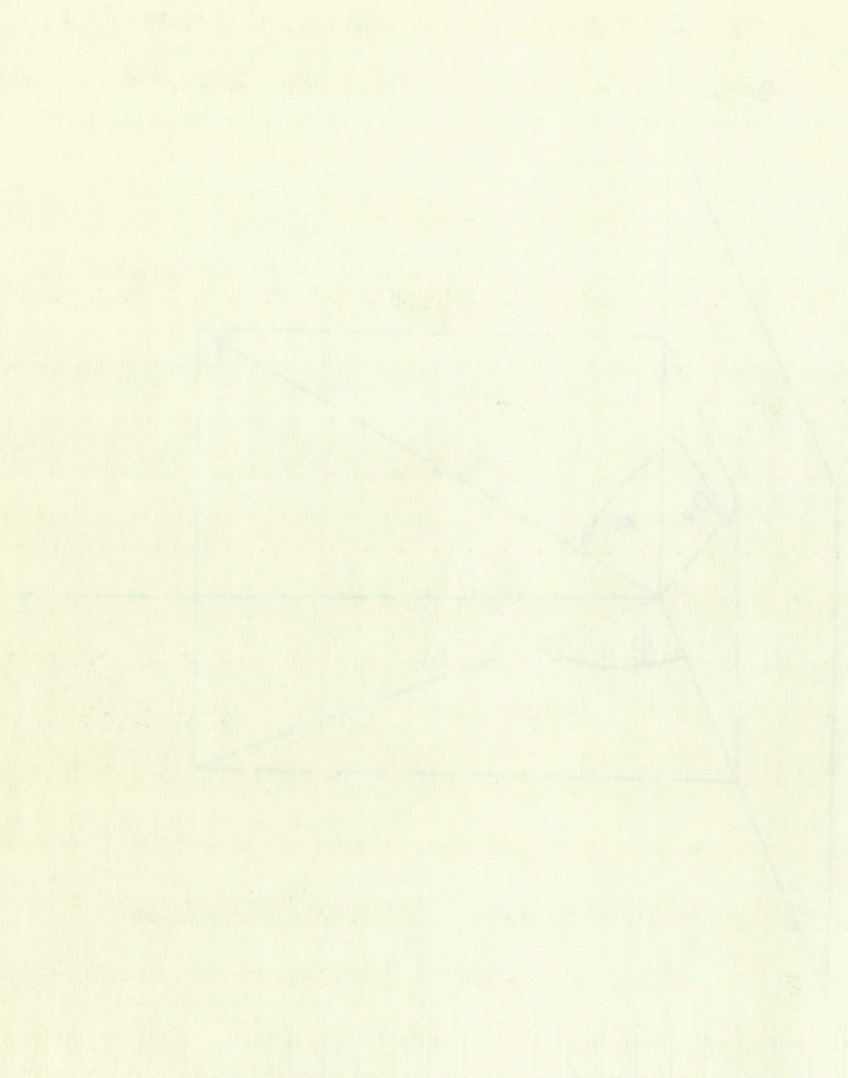
2) Experimental Determination of the Distribution

To determine the distribution of angles, it is necessary to reverse all of the angles from their original



Relation Between Observed Projected Angle And
Space Angles

Fig. 4



experiment. This was done by projecting each negative individually and selecting only those photographs that showed high energy electrons or a minimum of three nearly parallel tracks. The angles were measured from the vertical and averaged for each event. The tangent of each average angle was then squared and added. The mean square tangent was found to be

$$\frac{\quad}{2}$$

$$\tan^2 \theta_p = 0.186$$

$$\text{or } \bar{\theta}_p = 23.33^\circ$$

Employing equation (1), we obtain

$$n = 6.37.$$

4). Comparison with other Experiments.

The value of n obtained agrees favorably with other experiments performed to determine zenith angle distributions. Kraybill,¹⁰ using the $\cos^n \theta$ distribution, determined the mean zenith angle for mountain elevations to be approximately 20° . Other work by Daudin,¹⁶ Williams,¹⁷ Brown and McKay,¹⁸ using the same distribution, determined the mean zenith angle to be 30° , 25° , and 30° respectively, at various mountain altitudes.

One large deviation came from the work of Guseva, Zatsepsin, and Kristiansen¹⁴ in the U.S.S.R. at approximately 3860 meters. Using a cloud chamber and a hodoscope arrangement, they found the zenith angle to be very steep

experiment. This was done by varying the angle of the
individually and selecting the most appropriate angle
showed high energy efficiency at a distance of 1000 feet
parallel tracks. The angle was measured from the
and averaged for each angle. The average of each angle
angle was then selected as the best angle. The average
was found to be

$$\theta = 15.5^\circ$$

$$\theta = 15.5^\circ$$

Applying equation (1), we obtain

$$\theta = 15.5^\circ$$

4) Comparison with other investigators

The value of θ obtained above is compared with the
experiments performed by other investigators. The
Butler, Kuybil, and others have obtained values of
which the mean value is 15.5° . The values obtained by
approximately 15.5° . The values obtained by
Brown and Kelly, 15.5° . The values obtained by
the mean value is 15.5° . The values obtained by
at various angles of elevation.

One large deviation is found in the work of
Labadala, and Lalitha. The values obtained by
nearly 3800 meters. This is due to the
arrangement, compared the angles with the

with a value of n ranging from 7.5 to 13.5 with the most probable value being 11.

Experiments performed at Cornell University by K. Greisen¹⁵ show that the angular distribution there more nearly follows the distribution

$$\frac{x}{e^{\lambda}} (\sec\theta - 1)$$

where θ is the zenith angle and x the vertical depth of the atmosphere (at Cornell, 1006 gm./cm² .). This function gives a mean zenith angle of 27°.

The agreement between the various experiments is satisfactory in all cases except the one in the U.S.S.R.. In this case the discrepancy is strong and has not been explained; but the error quoted is large and the distribution somewhat uncertain. If this discrepancy can be ignored, the remaining agreement with the other values gives support of the method used in this experiment as a satisfactory means to study angular distributions of extensive air showers.

with a value of a percentage of 10. The value of the
probable value being 10.

Experimentally determined values for the
Grossen¹⁸ show that the value of the
nearly follows the distribution

$$y = \frac{1}{\sigma \sqrt{2\pi}} e^{-\frac{x^2}{2\sigma^2}}$$

where σ is the standard deviation and the
atmosphere (at 6000 ft. altitude) the mean
a mean kinetic energy of 10.

The agreement between the theoretical and
factory in all cases except the one in which
this case the distribution is not quite
but the error is small and the agreement
uncertain. It is therefore not possible
agreement with the theory which is expected
used in this experiment as a basis for
angular distribution of electrons and positrons.

V. ACKNOWLEDGEMENTS

The author is indebted to the following people for help and assistance throughout the course of this experiment, and for preparation and construction of most of the equipment prior to this experiment.

Dr. John R. Green, who suggested the experiment and designed and built the apparatus.

Dr. James R. Barcus, whose technical advice and encouragement were invaluable throughout the entire experiment.

Sandia Corporation, which donated the film used in the experiment.

EXPERIMENTAL

The author is indebted to the following for their help and assistance throughout the course of this study: Dr. J. H. ... and for providing the ... equipment prior to this experiment.

Dr. John R. ... who assisted in the experiments and analysis.

REFERENCES

Dr. James R. ... were investigated with the ... Sandia Corporation, ... experiment.

VI. REFERENCES

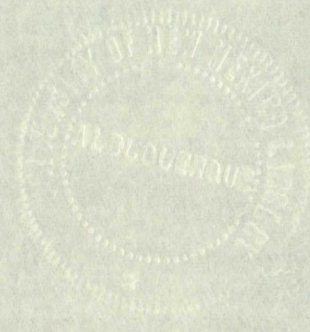
- 1). Rossi, Bruno, High Energy Particles, (Prentice Hall, 1956).
- 2). Kamata, K. and Nishimura, J., "The Lateral and the Angular Structure Functions of Electron Showers", Supplement of the Progress of Theoretical Physics, 6 (1958).
- 3). Greisen, K., "The Extensive Air Showers", Progress in Cosmic Ray Physics, Vol. III (1956).
- 4). Kenney, J. F., "A Cloud Chamber Study of Penetrating Showers in Aluminum, Copper, and Lead", Unpublished Doctoral Dissertation, University of New Mexico, 1957.
- 5). Janossy, L., Cosmic Rays, (Oxford-Press, 1948).
- 6). Green, J. R. and Barcus, J. R., "Size-Spectrum of Extensive Air Showers of the Cosmic Radiation", II Nuovo Cimento, 14 (1959).
- 7). Galbraith, W., Extensive Air Showers, (Academic Press Inc., 1958).
- 8). Roberg, J. and Nordheim, L. W., Physical Review, 75 (1949).
- 9). Ivanenko, I. P., "Cascade Curves From Electrons and Photons in Lead", Soviet Physics, Vol.1 (1956).
- 10). Kraybill, H. L., Physical Review, 93 (1954).
- 11). Bassi, Clark and Rossi, Physical Review, 92 (1953).
- 12). Cresti, M., II Nuovo Cimento, 10 (1953).
- 13). Barcus, J. R., "Size-Spectrum and Lateral Distribution of Electronic Energies for Extensive Air Showers", Unpublished Doctoral Dissertation, University of New Mexico, 1961.
- 14). Guseva, Zatssepsin, and Khristiansen, "On the Zenith Angle Distribution of High-Energy Extensive Air Showers", Soviet Physics, 35 (1959).
- 15). Greisen, K., "Absorption Length Versus Size of Extensive Air Showers", Proceedings of the Moscow Cosmic Ray Conference, Vol. III (1960).

I. ...

- 1) Rossi, Bruno, ... (1930).
- 2) Kamada, I., ... (1931).
- 3) Griesner, L., ... (1932).
- 4) Kamey, T., ... (1933).
- 5) Janovsky, J., ... (1934).
- 6) Green, E., ... (1935).
- 7) Gelstein, G., ... (1936).
- 8) Robert, J. and Verjast, J., ... (1937).
- 9) Iwanenko, I. I., ... (1938).
- 10) Brazdil, J., ... (1939).
- 11) Batai, ... (1940).
- 12) Cresti, M., ... (1941).
- 13) Barons, J. E., ... (1942).
- 14) Gusev, ... (1943).
- 15) Griesner, L., ... (1944).

- 16). Daudin, J., Physical Radium, 6 (1945).
- 17). Williams, R. W., Physical Review, 74 (1948).
- 18). McKay, A. S., Physical Review, 77 (1950).

STATE COLLEGE
LIBRARY
UNIVERSITY OF PENNSYLVANIA



- 16) Daudin, J., *Physiol. Rev.*, 1944.
- 17) Williams, R. A., *Physiol. Rev.*, 1944.
- 18) Jones, A. S., *Physiol. Rev.*, 1944.

COLLECTION
 EVERETT
 NORTH'S



COLLEGE COLLEGE
EZEVASE
MILITARY UNIT

MILERS FIELDS
EXETER
COTTON CONTAINERS

